Article:
Thorp-Greenwood, F, Brennan, AD, Oldknow, S et al. (2017) Tris-N-alkylpyridinium-functionalised cyclotriguaiacylene hosts as axles in branched [4]pseudorotaxane formation. Supramolecular Chemistry, 29 (6). pp. 430-440. ISSN: 1061-0278

https://doi.org/10.1080/10610278.2016.1265120

Tris-*N*-alkylpyridinium-functionalised cyclotriguaiacylene hosts as axles in branched [4]pseudorotaxane formation.

Flora L. Thorp-Greenwood, Alexander D. Brennan, Samuel Oldknow, James J. Henkelis, Katie J. Simmons, Colin W. G. Fishwick and Michaele J. Hardie.*

School of Chemistry, University of Leeds, Leeds LS2 9JT, UK.

m.j.hardie@leeds.ac.uk

Tris-*N*-alkylpyridinium-functionalised cyclotriguaiacylene hosts as axles in branched [4]pseudorotaxane formation

A series of [4]pseudorotaxanes composed of three-way axle threads based on the cyclotriguaiacylene family of crown-shaped cavitands and three threaded macrocyclic components has been achieved. These exploit the strong affinity for electron-poor alkyl-pyridinium units to reside within the electron-rich cavity of macrocycles, in this case dimethoxypillar[5]arene (DMP). The branched [4]pseudorotaxane assemblies $\{(DMP)_3 \cdot L\}^{3+}$,where L = *N*-alkylated derivatives of the host molecule (±)-*tris*-(isonicotinoyl)cyclotriguaiacylene, were characterised by NMR spectroscopy and mass spectrometry, and an energy-minimised structure of $\{(DMP)_3 \cdot$(*tris*-(*N*-propyl-isonicotinoyl)cyclotriguaiacylene)$\}^{3+}$ was calculated. Crystal structures of *N*-ethyl-isonicotinoyl)cyclotriguaiacylene hexafluorophosphate and *N*-propyl-isonicotinoyl)cyclotriguaiacylene hexafluorophosphate each show 'hand-shake' self-inclusion motifs occurring between the individual cavitands.

Keywords: mechanically interlocked molecules; pillar[5]arene; cyclotriveratrylene

Introduction

Mechanically interlocked molecules have attracted great interest, both as examples of interesting chemical architectures and as the control of motion within them may lead to applications in molecular machinery.[1,2] Examples include nanoscopic stimuli-responsive molecular shuttles,[3] molecular elevators,[4] muscle prototypes[5] and, most recently, a molecular pulley.[6] Mechanically interlocked molecules, such as catenanes and rotaxanes, are characterised by mechanical bonds where interlocking of molecular components with no covalent chemical bonds between them occurs. A rotaxane is composed of an axle-like component which threads through a macrocyclic wheel component with de-threading prevented by bulky end groups on the axle.[2]

Threading is often achieved through the manipulation of molecular recognition interactions between the components, where electrostatic interactions, π-π stacking and hydrogen bonding, etc. act to orient the individual components favourably prior to the mechanical bond formation. A pseudorotaxane is often a precursor to a rotaxane and has no physical barrier to de-threading. A common molecular recognition motif that is employed for pseudorotaxanes and rotaxanes is the combination of a positively charged alkyl-pyridinium – usually in the form of a *bis*-paraquat or alkane-linked bis(pyridinium) – with an electron-rich macrocyclic host such as a dibenzocrown ether [3,7] or, more recently, with pillar[5]arene.[8-12] Pillararenes have been extensively researched since their discovery in 2007.[8] Their composition is similar to that of a calixarene, however the 1,4-dimethoxybenzene units are bridged at the 2- and 5-positions as opposed to the 2- and 6-positions.[9] The inner cavity of pillar[5]arene is *ca.* 5 Å and electron rich,[9] making it making it well-suited for the complexation of shape-specific and electron-poor guest molecules.

Molecular hosts such as crown ethers, calixarenes, cucurbiturils and pillararenes have been frequently employed as the comprise the wheel component of pseudorotaxanes or rotaxanes.[2] Here, however, we report the use of a functionalised molecular host as an axle component in the formation of [4]pseudorotaxanes. Branched [4]pseudorotaxanes and rotaxanes have been previously reported with multi-armed axle components based either on a substituted 1,3,5-benzene [13] or a boroxine core,[14] and also with a tritopic wheel component.[15] Here we utilise the pyramidal-shaped host cyclotriguaiacylene as the scaffold for the branched tritopic axle, and combine with pillar[5]arene as the wheel component. Cyclotriguaiacylene (CTG) is a chiral host molecule that forms part of the cyclotriveratrylene family, Figure 1.[16] The hydroxyl groups are easily functionalised, and there is a rich chemistry of tritopic CTG extended-

arm CTG derivatives that have found great utility in host-guest chemistry and in the construction of both organic and metal-organic cages and assemblies.[16-18] There are few examples of molecular hosts being used as structured branched axles for pseudorotaxane or rotaxane formation, the best known are the tetra[2]rotaxanes reported by Böhmer and co-workers which are capsule-like heterodimers with urea-axle functionalisation on one calix[4]arene.[19]

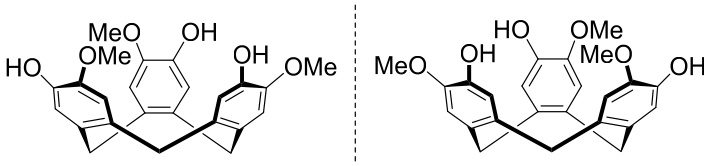

(±)-cyclotriguaiacylene (CTG)

Figure 1: Enantiomers of cyclotriguaiacylene

Results and Discussion

Tritopic branched-axle species were synthesised through the *N*-alkylation of (±)-*tris*-(isonicotinoyl)cyclotriguaiacylene. *Tris*-(isonicotinoyl)cyclotriguaiacylene has been previously reported as a ligand for crystalline coordination polymers [20,21] and cage-species.[18] *N*-alkylation was achieved through the reaction of *tris*-(isonicotinoyl)cyclotriguaiacylene with an excess of the appropriate alkyl bromide in the presence of KI, to give cationic cavitand molecules with three *N*-ethyl-pyridinium (**L1**$^{3+}$), *N*-propyl-pyridinium (**L2**$^{3+}$), *N*-butyl-pyridinium (**L3**$^{3+}$) and *N*-octyl-pyridinium (**L4**$^{3+}$) moieties in good yields, Scheme 1. Finkelstein conditions were used, employing sub-stoichiometric KI as the nucleophilic catalyst, which rendered the desired *N*-alkyl-pyridinium compounds as a mixture of bromide and iodide salts. The halide counter-anions were exchanged for hexafluorophosphate in order to improve the solubility of these charged compounds in common organic solvents, Scheme 1.

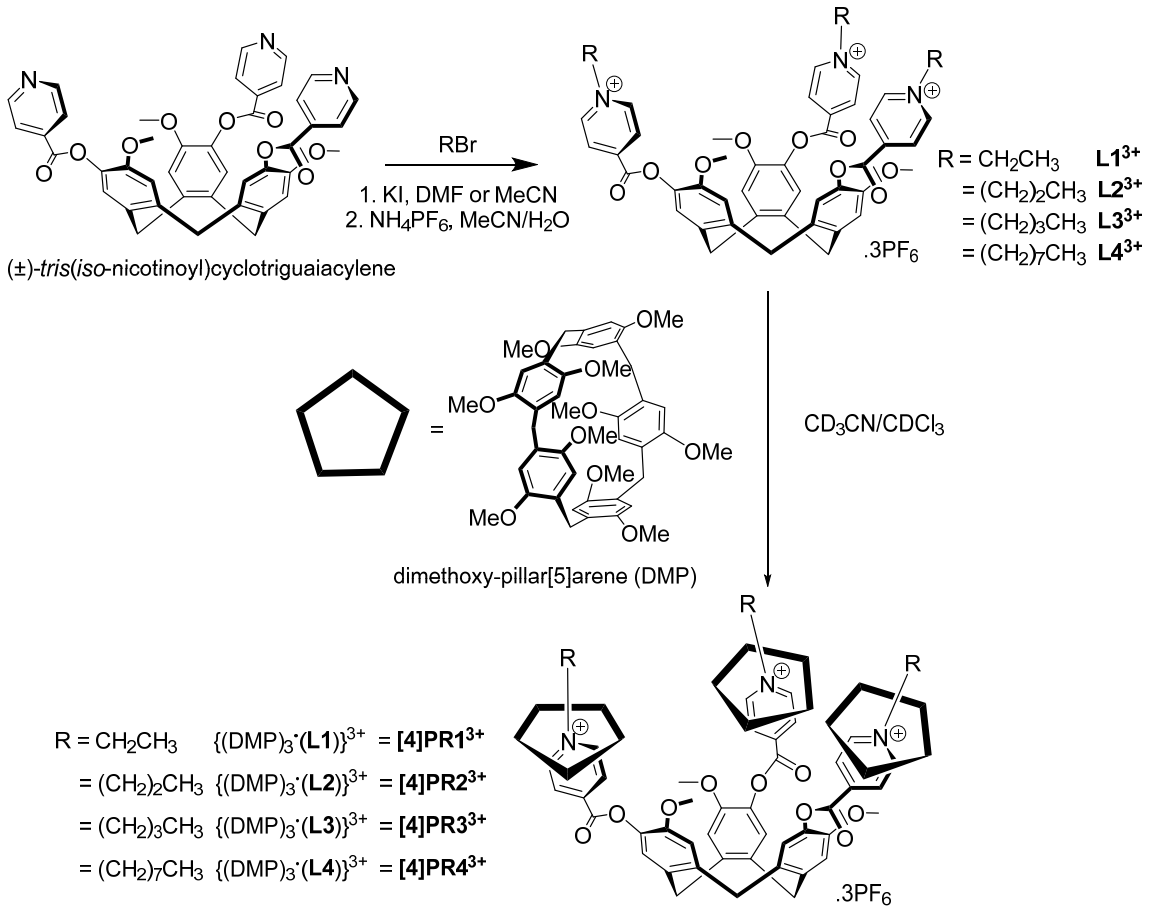

Scheme 1. Synthesis of tris-(N-alkyl-isonicotinoyl)cyclotriguaiacylene species and subsequent [4]pseudorotaxane formation ([4]PR) with dimethoxypillar[5]arene.

Single crystals suitable for X-ray structural analysis were obtained for the PF_6^- salts of (±)-*tris*-(*N*-ethyl-isonicotinoyl)cyclotriguaiacylene $\mathbf{L1}^{3+}$ and (±)-*tris*-(*N*-propyl-isonicotinoyl)cyclotriguaiacylene $\mathbf{L2}^{3+}$, with the structure of the former determined using data from synchrotron radiation. The structure of compound $\mathbf{L1}\cdot 3PF_6$ was solved in space group *C*2/*c* and consists of one $\mathbf{L1}^{3+}$ cation in the asymmetric unit. The $\mathbf{L1}^{3+}$ cations form self-inclusion pairs in the solid state, where an ethyl group of one cation behaves as a guest species for an adjacent cation and *vice versa* to form a "hand-shake" motif, Figure 2b. Within the pair the terminal propyl $-CH_3$ groups are directed almost exactly over the centre of the cavitand's molecular cavities. This hand-shake motif is

commonly seen for cyclotriguaiacylene derivatives,[22] as well as for other types of bowl-shaped host molecules.[23] In this case, however, the hand-shake is homochiral rather than occurring between enantiomeric pairs which is the more common observation. The terminal methyl group sits in the cavity at C···aromatic ring centroid separations between 3.57 and 4.16 Å. A notable aspect of this association is that it is occurring between cations, albeit with an 8.3 Å separation between the pyridinium N-atoms. Within the lattice there are even closer associations between *N*-ethyl-pyridinium moieties of adjacent cations, Figure 2c, with pairwise C_{methyl}···aromatic ring centroid separation of 3.74 Å. The cations account for ca. 50% of the unit cell volume, (see supplementary information for additional figures) and the crystal lattice also contains PF_6^- anions and is likely to contain solvent which could not be located in the difference map due to weak diffraction.

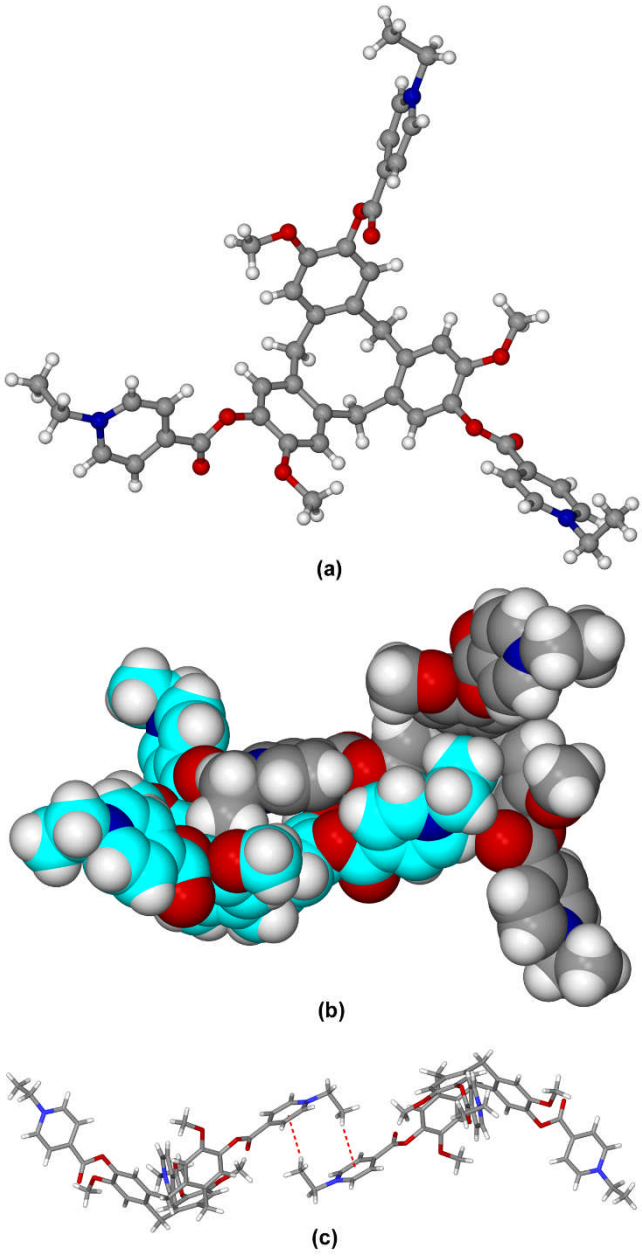

Figure 2. From the X-ray structure of ***L1***$\cdot 3PF_6$*. (a)* $\boldsymbol{L1}^{3+}$ *cation of the asymmetric unit; (b) hand-shake pair of cations in space-filling mode, highlighting the manner in which the ethyl groups are directed into the cavity of an adjacent host; (c) pair-wise C-H···π interaction between N-ethyl-pyridinium groups.*

The structure of complex $\mathbf{L2}\cdot 3PF_6\cdot 2(CH_3CN)\cdot 2(H_2O)$ was solved in space group *C*2/c and the asymmetric unit comprises two enantiomers of $\mathbf{L2}^{3+}$, one of which was refined as disordered (see supplementary material), four acetonitrile positions,

disordered water and ordered and disordered PF_6^- positions. As for **L1**·3PF_6 the cations form self-inclusion motifs. However, here a tetrameric rather than pair-wise association is observed. Each **L2**$^{3+}$ cation acts as a host for one *N*-propyl-pyridinium group of an adjacent **L2**$^{3+}$ cavitand of opposite chirality, and one of its three *N*-propyl-pyridinium groups occupies the guest position for a further **L2**$^{3+}$ host, also of opposite chirality. These associations lead to a cyclic tetrameric arrangement, Figure 3b. Here it is the α-CH_2- group rather than the terminal methyl that forms the host-guest association with the cavitand bowl, at distances indicative of weak C-H···π hydrogen bonding (C···ring centroid separations between 3.49 and 3.84 Å). Packing of the **L2**$^{3+}$ cavitand molecules creates circular channels which are occupied by PF_6^- and solvent molecules (see supplementary information).

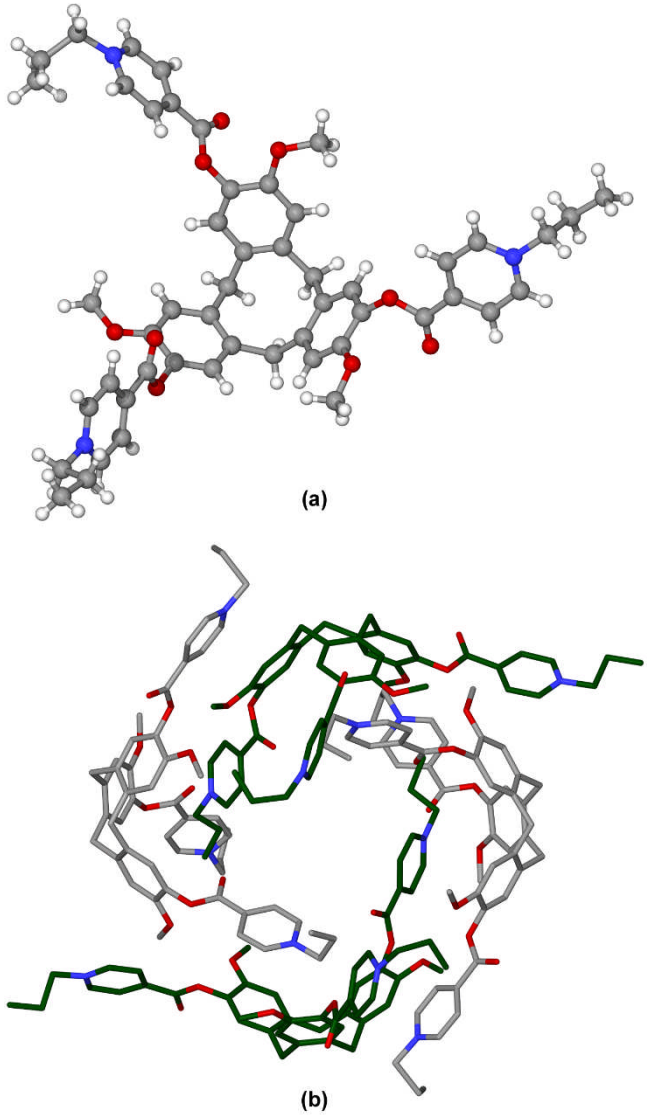

Figure 3. From the X-ray structure of ***L2***$\cdot 3PF_6 \cdot 2(CH_3CN) \cdot 2(H_2O)$*. (a) One* $\mathbf{L2}^{3+}$ *cation; (b) tetrameric hand-shake association with different* $\mathbf{L2}^{3+}$ *enantiomers in different shadings. Disordered propyl and N-propyl-pyridinium groups shown in a single position, and hydrogen atoms omitted for clarity.*

[4]Pseudorotaxane formation using the *tris*-(*N*-alkylated-isonicotinoyl)cyclotriguaiacylene cavitands $L \cdot 3PF_6$, where L = **L1-L4**, was investigated using dimethoxypillar[5]arene (DMP) as the macrocyclic wheel component. For each system the L^{3+} axle was dissolved in d_3-MeCN, and a solution containing three equivalents of dimethoxypillar[5]arene in *d*-chloroform was added. The solutions were

heated gently to ensure full dissolution of the components, then cooled before ^{1}H NMR spectroscopy and mass spectrometry were employed to confirm the formation of the [4]pseudorotaxane associations in solution, Scheme 1.

In all cases electrospray mass spectrometry (ES-MS) gave excellent evidence of formation of the [4]pseudorotaxane species $\{(DMP)_3\cdot(\mathbf{L1})\}^{3+}$ (= $\mathbf{[4]PR1}^{3+}$), $\{(DMP)_3\cdot(\mathbf{L2})\}^{3+}$ (= $\mathbf{[4]PR2}^{3+}$), $\{(DMP)_3\cdot(\mathbf{L3})\}^{3+}$ (= $\mathbf{[4]PR3}^{3+}$), and $\{(DMP)_3\cdot(\mathbf{L4})\}^{3+}$ (= $\mathbf{[4]PR4}^{3+}$). Mass spectrometry of the solutions of the 3:1 DMP:cavitand axle mixtures clearly show peaks corresponding to the mass of one cavitand axle combined with three dimethoxypillar[5]arene macrocycles, namely: $\mathbf{[4]PR1}^{3+}$ *m*/*z* = 1020.7910, $\mathbf{[4]PR2}^{3+}$ *m*/*z* = 1035.1386, $\mathbf{[4]PR3}^{3+}$ *m*/*z* = 1049.4812, $\mathbf{[4]PR4}^{3+}$ *m*/*z* = 1105.2189. All spectra also have *m*/*z* peaks corresponding to the unthreaded L^{3+} species. The high resolution mass spectrum obtained for the 3:1 mixture of DMP and $\mathbf{L3}\cdot 3PF_6$ is shown in Figure 4. As well as the peak corresponding to $\mathbf{[4]PR3}^{3+}$, it shows a series of 3^+ peaks corresponding to two, one and no DMP macrocycles threaded to the $\mathbf{L3}^{3+}$ cavitand, and shows no other products of self-assembly. The spectrum obtained for DMP and $\mathbf{L4}\cdot 3PF_6$ shows a similarly simple pattern of $\{(DMP)_n\cdot(\mathbf{L4})\}^{3+}$ species where n = 0-3 (see supplementary information). The spectra for the mixtures of DMP with $\mathbf{L1}\cdot 3PF_6$ or $\mathbf{L2}\cdot 3PF_6$ are more complicated (see supplementary material). They show a variety of charge states where one or two PF_6^- counter-anions are associated with the cation, for example the species $\{\mathbf{[4]PR2}\cdot PF_6\}^{2+}$ (*m*/*z* 1625.1895) is observed, along with the partially threaded$\{(DMP)_2\cdot(\mathbf{L2})\cdot PF_6\}^{2+}$ and $\{(DMP)\cdot(\mathbf{L2})\cdot PF_6\}^{2+}$ species.

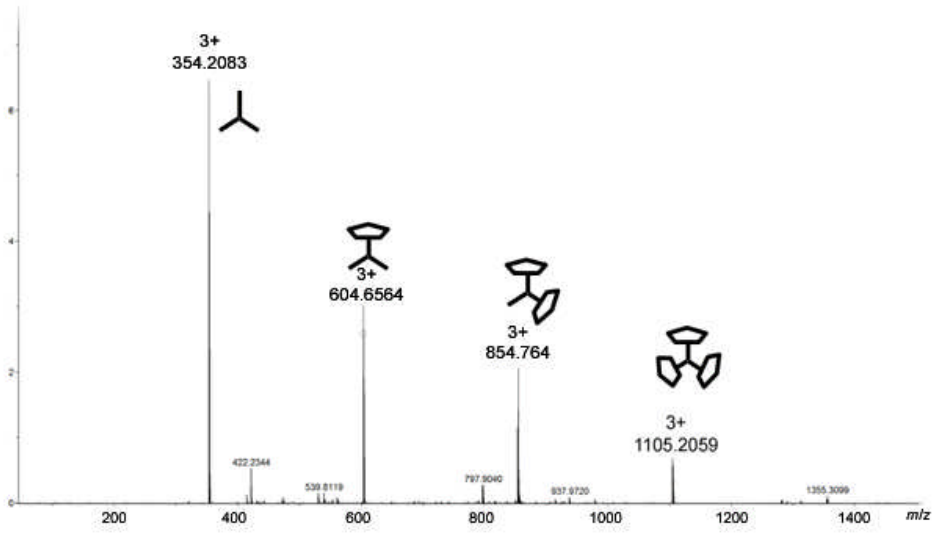

Figure 4. High-resolution Electrospray Mass spectrum of $CD_3CN/CDCl_3$ solution of 1:3 ***L4***$\cdot 3PF_6$ *and DMP, showing formation of* $\{(DMP)_3 \cdot \boldsymbol{L4}\}^{3+}$ *(=* $\boldsymbol{[4]PR4}^{3+}$*) at m/z 1105.2059 (calc 1105.2157), along with* $\{(DMP)_2 \cdot \boldsymbol{L4}\}^{3+}$ *at m/z 854.7674 (calc 854.7678),* $\{(DMP) \cdot \boldsymbol{L4}\}^{3+}$ *at m/z 604.6564 (calc 604.6543), and* $\boldsymbol{L4}^{3+}$ *at m/z 354.2083 (calc 354.2064).*

^{1}H NMR studies also support formation of the [4]pseudorotaxane species **[4]PR1**$^{3+}$ - **[4]PR4**$^{3+}$ with chemical shifts and through-space interactions observed consistent with those previously reported for other pillar[5]arene-alkyl-pyridinium systems.[8,12] In all cases the cavitand retained C_3-symmetry in solution and the pyridinium and alkyl protons of the cavitand axles showed chemical shift changes indicative of encapsulation by the dimethyoxy-pillar[5]arene macrocycles, Figure 5. In **[4]PR1**$^{3+}$, Figure 5a, significant upfield shifts were observed for the N-CH_2 α-protons of the ethyl chains (H^i) with a shift of 0.22 ppm, whilst the terminal CH_3 (H^h) shows a smaller shift of 0.14 ppm. The *ortho*-pyridyl hydrogen environment (H^a) at 8.92 ppm shows a much larger upfield shift of 0.49 ppm, indicating that those protons experience significant shielding from the aromatic ring, whilst the *meta*-hydrogen environment (H^b) shows little movement (0.07 ppm). Instead it broadens out into a singlet and this loss of

splitting has been observed in other systems.[8,10] Similar shifts are observed for **[4]PR2**$^{3+}$ and **[4]PR3**$^{3+}$, Figure 5b/c. Both systems showed significant upfield shifting of the H^a *ortho* proton of the pyridinium (0.43 ppm for **[4]PR2**$^{3+}$, 0.42 ppm for **[4]PR3**$^{3+}$) and almost no shifting of the H^b *meta* protons. As before, the highest upfield shift observed in the alkyl chains is for the α-protons (0.33 ppm for **[4]PR2**$^{3+}$ and 0.25ppm for **[4]PR3**$^{3+}$), with smaller shifts observed for the protons nearing the terminus. The terminal methyl protons in both cases show only a small shift of ca. 0.05 ppm, suggesting that the alkyl chain has passed through the macrocycle and the terminal group is not encapsulated.

While there is clear indication of [4]pseudorotaxane formation by ESI-MS for the octyl-appended **L4**$^{3+}$, the chemical shifts observed by ^{1}H NMR are somewhat smaller than was observed for the pseudorotaxanes with the shorter alkyl-chain species **L1**-**L3**$^{3+}$. The strongest upfield shifts correspond to the *ortho* proton (H^a) associated with the pyridinium moieties, and the α-protons (H^i) of the octyl group which appear at 8.92 and 4.62 ppm respectively in the free axle and 8.76 and 4.49 ppm in the **[4]PR4**$^{3+}$ assembly, Figure 5d. The β-protons (H^j) of the octyl chains show very little shifting and there are no significant shifts through the rest of the chain. Overall, it is evident that the shorter chain axles (**L1**$^{3+}$-**L3**$^{3+}$) exhibit much larger proton shifts than the longer octyl appended axle **L4**$^{3+}$. This may be due to the additional flexibility of the octyl chain resulting in weaker binding due to more degrees of freedom being inhibited on threading, or an increased degree of fluxionality of the DMP along the alkyl chain.

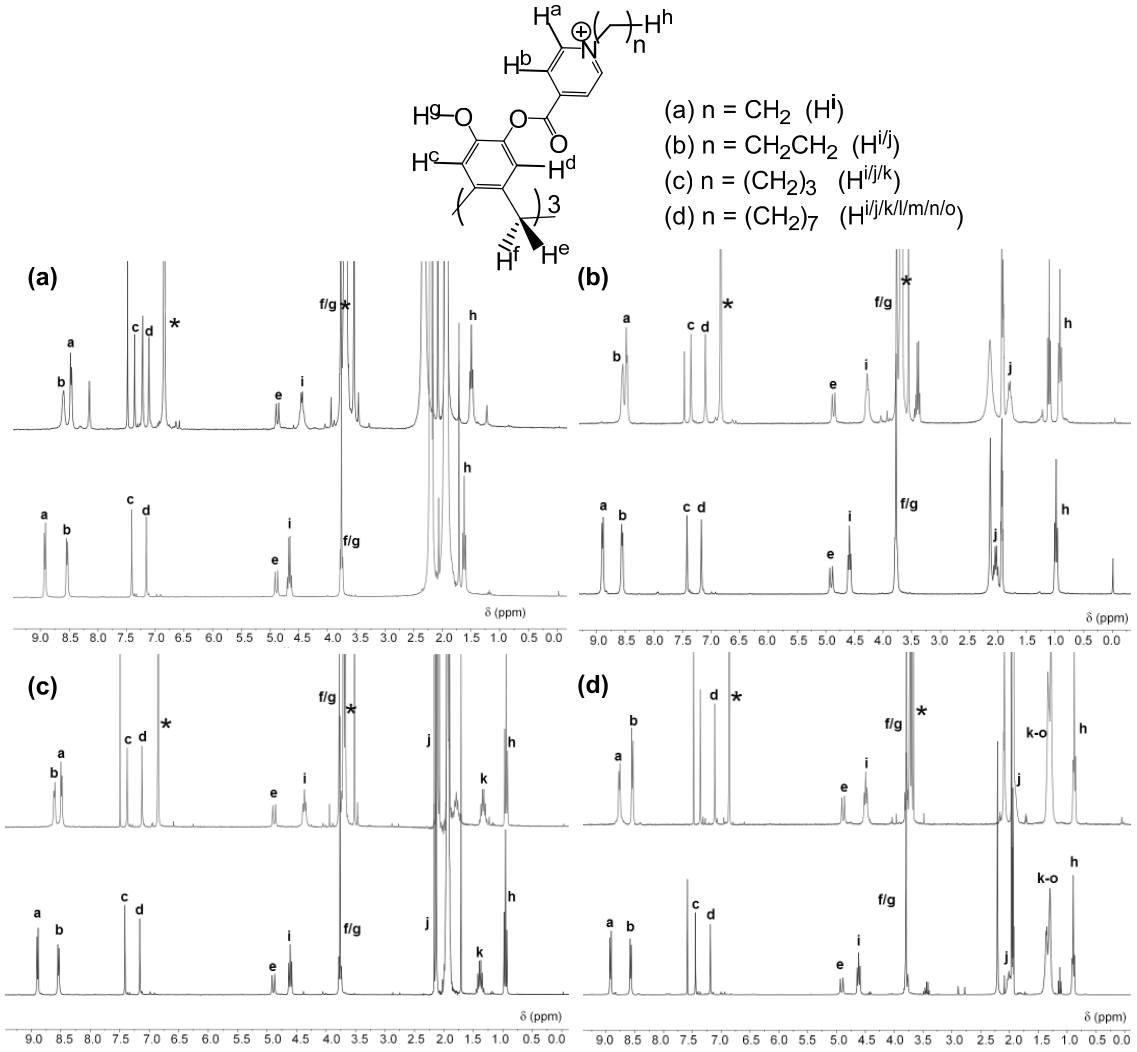

Figure 5: ^{1}H NMR (300 MHz) studies for the formation of PF_6^- salts of pseudorotaxanes ***[4]PR1^{3+}-[4]PR4^{3+}****: (a) {(DMP)$_3$·(**L1**)}$^{3+}$ (= **[4]PR1**$^{3+}$) upper spectrum and **L1**$^{3+}$ lower spectrum; (b) {(DMP)$_3$·(**L2**)}$^{3+}$ (= **[4]PR2**$^{3+}$) upper spectrum and **L2**$^{3+}$ lower spectrum; (c) {(DMP)$_3$·(**L3**)}$^{3+}$ (= **[4]PR3**$^{3+}$) upper spectrum and **L3**$^{3+}$ lower spectrum; (d) {(DMP)$_3$·(**L4**)}$^{3+}$ (= **[4]PR4**$^{3+}$) upper spectrum and **L4**$^{3+}$ lower spectrum. In all cases signals from DMP are denoted by asterisks (*).*

2D NMR experiments were also conducted on the pseudorotaxane species. Weak through-space interactions were observed for all the pseudorotaxanes in the

NOESY spectra; the NOESY spectrum of [**4]PR1**$^{3+}$ (={$(DMP)_3$·(**L1**)}$^{3+}$) is shown in Figure 6. Weak interactions are observed between the H^i *ortho* protons on the pyridyl ring of the axle (**a**) and the aromatic DMP protons (H^1). Further weak coupling is also seen between the terminal ethyl protons (H^h) and the methoxy protons on DMP (H^3). NOESY spectra for the other pseudorotaxanes [**4]PR2**$^{3+}$ - [**4]PR4**$^{3+}$ are shown in the supplementary material. Literature values for association constants for 1:1 complexes of DMP with alkylated pyridinium guest species are consistently ca. 1-2 x 10^3 M^{-1}.[8,12] Given these modest expected binding constants and the symmetrical nature of the NMR spectra a mixture of [2]-, [3]- and [4]-pseudorotaxanes species may exist in solution and these are likely to be in rapid exchange on the NMR timescale.

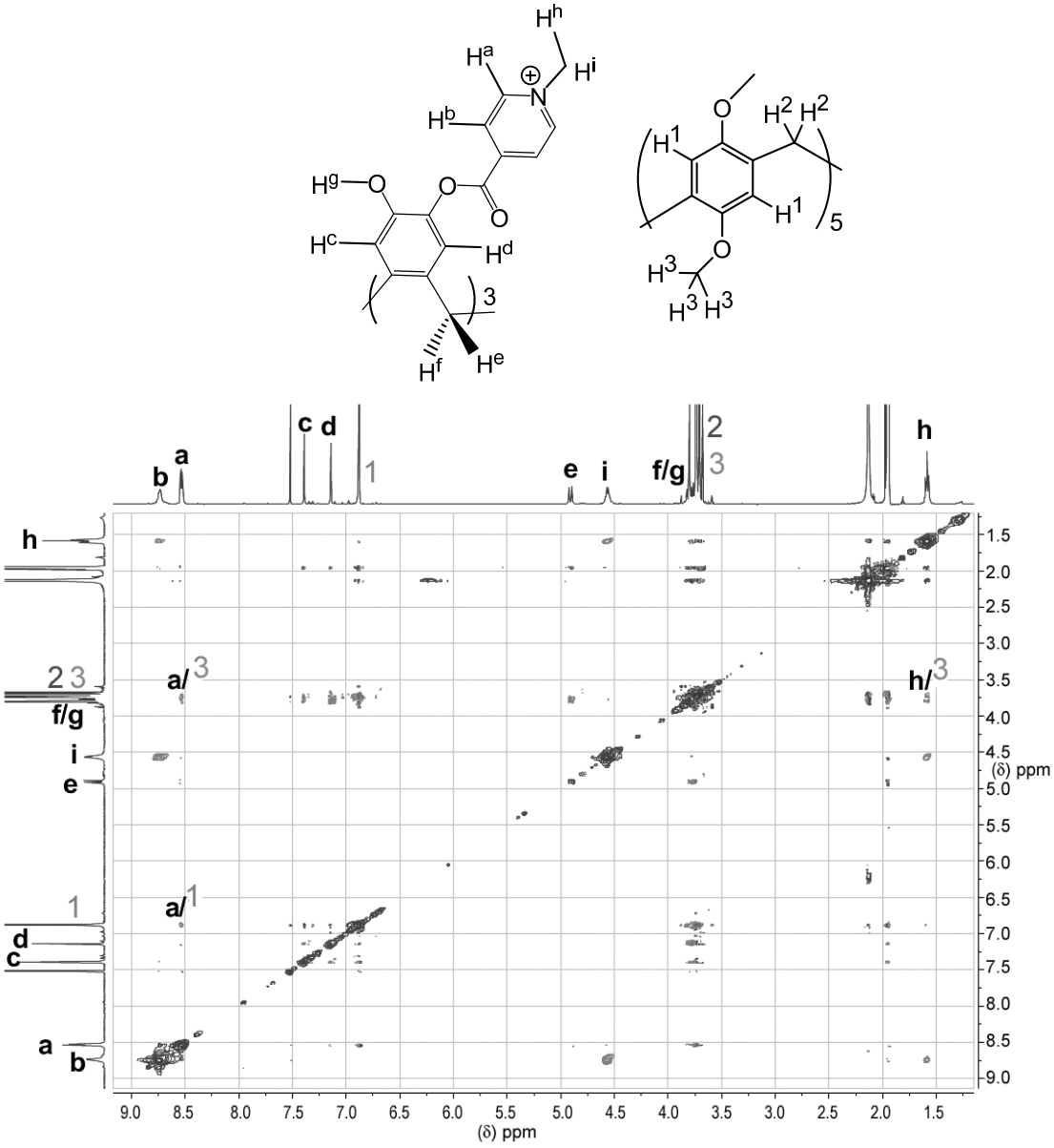

Figure 6. NOESY spectrum of ***[4]PR1***$^{3+}$ *in* d_3*-MeCN/*$CDCl_3$ *showing through-space interactions between axle* ***L1***$^{3+}$ *and DMP at three points.*

Attempts to crystallise the [4]pseudorotaxanes were unsuccessful as changes to solvent composition through slow evaporation invariably led to the crystallisation of dimethoxypillar[5]arene, which is only sparingly soluble in the acetonitrile co-solvent.

An energy-minimised structure of the [4]pseudorotaxane **[4]PR2**$^{3+}$ was therefore calculated to shed light on the assembled structure. This model shows that the three pseudorotaxane associations fit well with the minimised **L2**$^{3+}$ structure, with no steric clashes with either themselves or the ligand, Figure 7. The most favourable binding sites for the macrocycles are located directly over the cationic nitrogen of the pyridinium arms with the methoxy-groups at both ends of the macrocycle residing either side of the nitrogen position so to best interact with this electron-poor donor. The structure shows approximate C_3-symmetry with each *N*-propyl-isonicotinonyl arm extended away from the cavity and each DMP macrocycle threading parallel to the π-system of the pyridinium unit on each arm. This is in keeping with the ^{1}H NMR studies where the strongest upfield shifts suggest that the electron-poor pyridinium group and the α-CH_2 of the alkyl chain are enveloped within the electron-rich macrocycle.

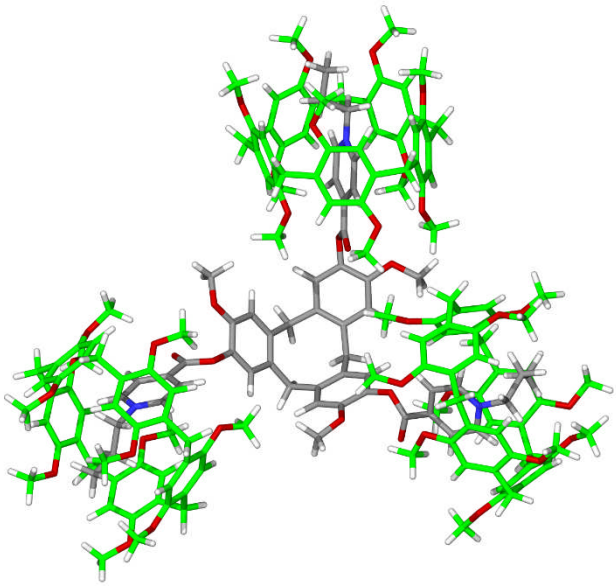

Figure 7. Energy-minimised structure of $\{(DMP)_3 \cdot (\mathbf{L2})\}^{3+}$ ***(= [4]PR2***$^{3+}$*).*

Experimental

Synthesis

Dimethoxypillar[5]arene (DMP) [8] and (±)-*tris*(isonicotinoyl)cyclotriguaiacylene [20] were synthesised by literature methods. All other chemicals were obtained from commercial sources and were used without further purification. ^{1}H NMR spectra were recorded by automated procedures on a Bruker DPX 300 MHz NMR spectrometer. Electrospray mass spectra (ES-MS) were measured on a Bruker Maxis Impact instrument in positive ion mode. Infra-red spectra were recorded as solid phase samples on a Bruker ALPHA Platinum ATR. Elemental analyses were performed on material that had been washed with diethyl ether, subsequently dried at 80-90 ˚C under vacuum and then exposed to the atmosphere.

(±)-*Tris*-(*N*-ethyl-isonicotinoyl)cyclotriguaiacylene halide L1·3X (±)-*Tris*-(isonicotinoyl)cyclotriguaiacylene (400 mg, 0.55 mmol) and potassium iodide (ca. 60 mg) were added to acetonitrile (65 ml). Bromoethane (2 ml, excess) was added and the mixture heated under reflux with stirring at 95 ºC for 88 hours. The resulting orange solution and suspension was filtered, and the solid washed with ether. The solid was extracted into minimal nitromethane, forming a yellow solution and leaving white potassium iodide behind. The solid was removed by filtration and ether was added slowly to the filtrate to induce precipitation. The solution was left to precipitate in the freezer, and the solid **L1**·3X (X= Br or I) collected by filtration as a yellow powder (280 mg, 0.40 mmol, 73%). HR-MS (ES^{+}) *m/z* 270.1129 (3+), $C_{48}H_{48}N_3O_9^{3+}$ requires 270.1125. ^{1}H NMR (300 MHz, dimethylsulfoxide-d_6) δ 9.40 (d, *J* = 7.0 Hz, 6H, H^{a}), 8.70 (d, *J* = 6.8 Hz, 6H, H^{b}), 7.67 (s, 3H, H^{c}), 7.37 (s, 3H, H^{d}), 4.97 (d, *J* = 13.3 Hz, 3H, H^{e}), 4.80 (q, *J* = 7.2 Hz, 6H, H^{i}), 3.79 (d, 3H, H^{f}) overlapped with 3.76 (s, 9H, H^{g}), 1.60

(t, J = 7.3 Hz, 9H, H^h). ^{13}C NMR (75 MHz, dimethylsulfoxide-d_6) δ 160.5 (C=O), 148.8 (pyridyl C *para* to N), 146.5 (pyridyl C *ortho* to N), 142.3 (quaternary aryl CTG), 139.4 (quaternary aryl CTG), 137.2 (quaternary aryl CTG), 132.0 (quaternary aryl CTG), 127.7 (pyridyl *meta* to N), 123.8 (aryl CTG C-H), 114.6 (aryl CTG C-H), 57.1 ($\underline{C}H_2CH_3$), 56.4 ($O\underline{C}H_3$), 34.9 ($H\underline{C}H$), 16.3 ($CH_2\underline{C}H_3$). FT-IR (cm^{-1}): 3113 (aromatic C-H), 3039 - 2937 (alkane C-H), 1742 (s, n) (C=O), 1642, 1615, 1575, 1508, 1457, 1400, 1324, 1281 (s, b) (aromatic C-N), 1205, 1178, 1138, 1115, 1070 (m, n) (C-O ester), 1047, 1004, 971, 941, 925, 866, 816, 798, 766, 743, 716, 702, 683, 660, 630, 616, 501, 454. Elemental analysis indicates isolated salt contains I^-, calculated for $C_{48}H_{48}N_3O_9I_3$ (%): C 48.38, H 4.06, N 3.53. Found: C 47.8, H 4.60, N 3.40.

(±)-*Tris*-(*N*-ethyl-isonicotinoyl)cyclotriguaiacylene hexafluorophosphate L1·3PF$_6$

L1·3X (100 mg) was dissolved in water (20 ml). Ammonium hexafluorophosphate (80 mg, excess) was added to exchange the halide ions resulting in oil formation. The oil was triturated for 10 minutes to give a very fine yellow solid, which was collected by filtration (80 mg, 0.064 mmol, 77 %). ^1H NMR (300 MHz, acetonitrile-d_3) δ 8.93 (d, J = 6.9 Hz, 6H, H^a), 8.54 (d, J = 6.6 Hz, 6H, H^b), 7.41 (s, 3H, H^c), 7.15 (s, 3H, H^d), 4.91 (d, J = 13.8 Hz, 3H, H^e), 4.65 (q, J = 7.3 Hz, 6H, H^i), 3.76 (d, J = 13.3 Hz, 3H, H^f), 3.76 (s, 9H, H^g), 1.61 (t, J = 7.3 Hz, 9H, H^h). Elemental analysis, calculated for $C_{48}H_{48}N_3O_9P_3F_{18}.2H_2O$ (%): C 44.98, H 4.09, N 3.28. Found: C 44.83, H 3.54, N 3.43.

(±)-*Tris*-(*N*-propyl-isonicotinoyl)cyclotriguaiacylene hexafluorophosphate L2·3PF$_6$

(±)-*Tris*(isonicotinoyl)cyclotriguaiacylene (200 mg, 0.28 mmol), potassium iodide (30 mg, 0.2 mmol) and 1-bromopropane (3 ml, excess) were added to *N*,*N*'-dimethylformamide (DMF, 10 ml). The mixture was heated at 120 °C with stirring for 60 hours. The reaction was then cooled to room temperature, and water (20 ml) was

added to precipitate the crude product as a yellow solid. This was collected and redissolved in acetonitrile (10 ml) and a saturated solution of ammonium hexafluorophosphate (182 mg, 1.1 mmol, 4 eq.) was added dropwise to the stirred solution giving **L2**·3PF_6 as an orange solid (255 mg, 0.19 mmol, 69 %). HR-MS (ES^+) *m/z* 1142.3138. $C_{51}H_{54}N_3O_9P_2F_6^+$ requires 1142.3127. ^{1}H NMR (300 MHz, acetonitrile-d_3) δ 8.90 (d, *J* = 6.6 Hz, 6H, H^a), 8.56 (d, *J* = 6.0 Hz, 6H, H^b), 7.43 (s, 3H, H^c), 7.18 (s, 3H, H^d), 4.91 (d, *J* = 13.8 Hz, 3H, H^e), 4.60 (t, *J* = 7.2 Hz, 6H, H^i), 3.78 (m, 12H, $H^{f/g}$), 2.04 (q, *J* = 7.5 Hz, 6H, H^j), 0.99 (t, *J* = 7.5 Hz, 9H, H^h). ^{13}C NMR (75 MHz, DMSO-d_6) δ 160.4 (C=O), 148.8 (pyridyl C *para* to N), 146.6 (pyridyl C *ortho* to N), 142.4 (quaternary aryl CTG), 139.4 (quaternary aryl CTG), 137.2 (quaternary aryl CTG), 132.0 (quaternary aryl CTG), 127.8 (pyridyl *meta* to N), 114.6 (aryl CTG C-H), 62.7 ($\underline{C}H_2$ α to N), 56.3 (O$\underline{C}H_3$), 35.0 (H$\underline{C}$H), 24.3 ($\underline{C}H_2$ β to N), 10.2 ($CH_2\underline{C}H_3$). FT-IR (cm^{-1}): 1754, 1645, 1615 (C-N), 1580, 1507, 1461, 1400, 1328, 1279, 1207, 833 (P-F). Elemental analysis, calculated for $C_{51}H_{54}F_{18}N_3O_9P_3$ (%): C 47.67, H 3.99, N 3.33. Found: C 47.56, H 4.23, N 3.26.

(±)-*Tris*-(*N*-butyl-isonicotinoyl)cyclotriguaiacylene hexafluorophosphate L3·3PF_6

(±)-*Tris*(isonicotinoyl)cyclotriguaiacylene (200 mg, 0.28 mmol), potassium iodide (30 mg, 0.2 mmol) and 1-bromobutane (3 ml, excess) were added to DMF (10 ml), and heated at 120 ºC with stirring for 60 hours. The reaction was then cooled to room temperature, and water (20 ml) was added to precipitate the crude product as a yellow solid. This was redissolved in acetonitrile (10 ml) and a saturated solution of ammonium hexafluorophosphate (182 mg, 1.1 mmol, 4 eq.) was added dropwise to the stirred solution to precipitate **L3**·3PF_6 as a brown solid (312 mg, 0.24 mmol, 88 %). HR-MS (ES^+) *m/z* 298.1437 (3+). $C_{54}H_{60}N_3O_9^{3+}$ requires 298.1438. ^{1}H NMR (300

MHz, nitromethane-d_3) δ 8.90 (d, J = 6.8 Hz, 6H, H^a), 8.53 (d, J = 6.6 Hz, 6H, H^b), 7.41 (s, 3H, H^c), 7.15 (s, 3H, H^d), 4.92 (d, J = 13.8 Hz, 3H, H^e), 4.60 (t, J = 7.5 Hz, 6H, H^i), 3.76 (s, 3H, H^f), 3.76 (s, 9H, H^f), 1.92 (p, J = 6 Hz, overlap with d_3-MeCN, 6H, H^g), 1.37 (h, J = 7.3 Hz, 6H, H^k), 0.95 (t, J = 7.3 Hz, 9H, H^h). ^{13}C NMR (75 MHz, nitromethane-d_3) δ 160.5 (C=O), 149.6 (pyridyl C *para* to N), 145.7 (pyridyl C *ortho* to N), 144.2 (quaternary aryl CTG), 139.6 (quaternary aryl CTG), 137.8 (quaternary aryl CTG), 132.1 (quaternary aryl CTG), 128.2 (pyridyl *meta* to N), 123.6 (aryl CTG C-H), 114.4 (aryl CTG C-H), 62.9 ($\underline{C}H_2$ α to N), 55.8 ($O\underline{C}H_3$), 35.3 ($H\underline{C}H$), 33.0 ($\underline{C}H_2$ β to N), 19.0 ($CH_2\underline{C}H_2CH_3$), 12.3 ($CH_2\underline{C}H_3$). FT-IR (cm^{-1}): 3021 - 2715 (C-H), 1752 (w, n) (C=O), 1685, 1608, 1537, 1505, 1450, 1403, 1385, 1370, 1335, 1281 (m, b) (aromatic C-N), 1206, 1176, 1136, 1099, 1068 (w, n) (C-O ester), 1032, 1003, 830 (s, b) (PF_6 stretch), 761, 738, 682, 634, 584, 556 (s, n) (PF_6 bend), 531, 506. Elemental analysis indicates $C_{54}H_{60}N_3O_9P_4F_{24}.0.5MeNO_2$ (%): C48.11, H 4.56, N 3.60. Found: C 47.73, H 4.10, N 3.38.

(±)-*Tris*-(*N*-octyl-isonicotinoyl)cyclotriguaiacylene hexafluorophosphate L4·3PF$_6$

(±)-*Tris*(isonicotinoyl)cyclotriguaiacylene (500 mg, 0.69 mmol) and potassium iodide were added to DMF (6 ml), and 1-bromooctane (2 ml, 10.6 mmol, 16 eq.) was added and the solution was heated at 100 ºC with stirring for 60 hours. The orange solution was precipitated with water and excess 1-bromooctane (a colourless oil) was decanted off and the resultant orange wax was re-dissolved in acetonitrile (10 ml) and excess solid NH_4PF_6 was added which induced the precipitation of an orange wax. The wax was dissolved in acetonitrile (10 ml) and was added to water (50ml) and extracted with $CHCl_3$ (3 x 50 ml). The organic layers were combined and evaporated. The solid was triturated in methanol (10 ml) and collected by filtration under suction and washed with ether to remove residual 1-bromooctane and leave the product as a pale yellow powder

(612 mg, 0.41 mmol, 59 % after salt exchange). HR-MS (ES^+) *m/z* 354.2058 (3^+). $C_{66}H_{84}N_3O_9^{3+}$ requires 354.2064. ^{1}H NMR (300 MHz, nitromethane-d_3) δ 8.93 (d, *J* = 9 Hz, 6H, H^a), 8.56 (d, *J* = 9 Hz, 6H, H^b), 7.48 (s, 3H, H^c), 7.19 (s, 3H, H^d), 4.93 (d, *J* = 15 Hz, 3H, H^e), 4.62 (t, *J* = 9 Hz, 6H, H^i), 3.80 (d, 3H, H^f) overlapped with 3.80 (s, 9H, H^f), 2.01 (m, 6H, H^j), 1.35 (m, 30H, H^{k-o}). 0.89 (t, *J* = 6 Hz, 9H, H^h). ^{13}C NMR (75 MHz, nitromethane-d_3) δ 160.6 (C=O), 149.6 (pyridyl C *para* to N), 146.1 (pyridyl C *ortho* to N), 144.0 (quaternary aryl CTG), 139.6 (quaternary aryl CTG), 137.8 (quaternary aryl CTG), 132.0 (quaternary aryl CTG), 128.1 (pyridyl *meta* to N), 123.6 (aryl CTG C-H), 114.4 (aryl CTG C-H), 62.8 ($\underline{C}H_2$ α to N), 55.8 ($O\underline{C}H_3$), 35.3 ($H\underline{C}H$), 31.4 ($\underline{C}H_2$ β to N), 28.6 (octyl $\underline{C}H_2$), 25.6 (octyl $\underline{C}H_2$), 22.3 (octyl $\underline{C}H_2$), 13.1 ($CH_2\underline{C}H_3$). FT-IR (cm^{-1}): 3118 - 3031 (aromatic C-H), 2926 - 2853 (alkane C-H), 1750 (s, n) (C=O), 1641, 1615, 1574, 1507, 1460, 1400, 1325, 1270 (s, b) (aromatic C-N), 1206, 1178, 1138, 1103, 1069 (m, n) (C-O ester), 1048, 1004, 924, 872, 816, 765, 744, 720, 682, 661, 639, 629, 547, 508. Elemental analysis calculated for $C_{66}H_{84}N_3O_9P_3F_{18}$ (%): C 52.91, H 5.65, N 2.80. Found: C 53.00, H 5.70, N 2.70.

[4]Pseudorotaxane formation

General procedure: Dimethoxypillar[5]arene (DMP) dissolved in $CDCl_3$ was added to a solution of a (±)-*tris*(*N*-alkyl-isonicotinoyl)cyclotriguaiacylene hexafluorophosphate dissolved in an equal quantity of d_3-acetonitrile with gentle heating to ensure dissolution of the DMP. ^{1}H NMR and ESI-MS data were collected on the cooled solutions.

{(DMP)$_3$·L1}·3PF$_6$ (= **[4]PR1·3PF$_6$**). ^{1}H NMR (300 MHz, CD_3CN:$CDCl_3$) δ 8.60 (s, 6H, H^b), 8.45 (d, *J* = 6 Hz, 6H, H^a), 7.36 (s, 3H, H^c), 7.11 (s, 3H, H^d), 6.84 (s, 10H, aryl-DMP), 4.88 (d, *J* = 15.0 Hz, 3H, H^e), 4.44 (q, *J* = 6.0 Hz, 6H, H^i), 3.77 (m, 12H, H^f, H^g) 3.70 (s, 30H, DMP-methoxy), 3.67 (s, 10H, CH_2-DMP), 1.49 (t, *J* = 9.0 Hz, 9H, H^h)

ppm. High-resolution Electrospray Mass spectrometry of $CD_3CN/CDCl_3$ solution of 1:3 **L1**·$3PF_6$ and DMP, showing formation of **[4]PR1**$^{3+}$ at *m*/*z* 1020.7910 (calc 1020.7873), along with {$(DMP)_2$·**L1.PF$_6$**}$^{2+}$ at *m*/*z* 1228.4931 (calc 1228.4931), {(DMP)·**L1.PF$_6$**}$^{2+}$ at *m*/*z* 853.3231 (calc 853.3229), {(DMP)·**L1**}$^{3+}$ at *m*/*z* 520.5610 (calc 520.5604) and **L1**$^{3+}$ at *m*/*z* 270.1141 (calc 270.1125).

{$(DMP)_3$·L2}·3PF$_6$ (= **[4]PR2·3PF$_6$**). ^{1}H NMR (300 MHz, CD_3CN:$CDCl_3$) δ 8.55 (d, *J* = 6.0 Hz, 6H, H^b), 8.47 (d, *J* = 6.0 Hz, 6H, H^a), 7.35 (s, 3H, H^c), 7.10 (s, 3H, H^d), 6.83 (s, 10H, aryl-DMP), 4.87 (d, *J* = 12.0 Hz, 3H, H^e), 4.28 (t, *J* = 6.0 Hz, 6H, H^i), 3.76 (m, 12H, H^f, H^g) 3.69 (s, 30H, DMP-methoxy), 3.67 (s, 10H, CH_2-DMP), 1.79 (m, 6H, C<u>H</u>$_2$ H^j), 0.92 (t, *J* = 6.0 Hz, 9H, H^h) ppm. Mass spectrometry of $CD_3CN/CDCl_3$ solution of 1:3 **L2**·$3PF_6$ and DMP, showing formation of **[4]PR2**$^{3+}$ at *m*/*z* 1035.1386 (calc 1035.1374), {**[4]PR2**·PF_6}$^{2+}$ at *m*/*z* 1625.1895 (calc 1625.1885), along with **L2**$^{3+}$ at *m*/*z* 284.1265 (calc 284.1281) and **L2.PF$_6$** $^{2+}$ at *m*/*z* 498.6754 (calc 498.6739).

{$(DMP)_3$·L3}·3PF$_6$ (= **[4]PR3·3PF$_6$**). ^{1}H NMR (300 MHz, CD_3CN:$CDCl_3$) δ 8.61 (d, *J* = 6.0 Hz, 6H, pyridyl *meta* to N), 8.49 (d, *J* = 6.0 Hz, 6H, pyridyl *ortho* to N), 7.38 (s, 3H, aryl CTG), 7.12 (s, 3H, aryl CTG), 6.85 (s, 10H, aryl-DMP), 4.87 (d, *J* = 12.0 Hz, 3H, <u>H</u>CH), 4.37 (t, *J* = 6.0 Hz, 6H, C<u>H</u>$_2$ α to N), 3.78 (m, 12H, H^f, H^g) 3.71 (s, 30H, DMP-methoxy), 3.68 (s, 10H, CH_2-DMP), 1.79 (m, 6H, C<u>H</u>$_2$ β to N), 1.33 (m, 6H, $CH_2C\underline{H}_2CH_3$), 0.94 (t, *J* = 6.0 Hz, 9H, $CH_2C\underline{H}_3$) ppm. High-resolution Electrospray Mass spectrometry of $CD_3CN/CDCl_3$ solution of 1:3 **L3**·$3PF_6$ and DMP, showing formation of **[4]PR3**$^{3+}$ at *m*/*z* 1049.1565 (calc 1049.1531), along with {$(DMP)_2$·**L3**}$^{3+}$ at *m*/*z* 798.7068 (calc 798.7052) and **L3**$^{3+}$ at *m*/*z* 298.1469 (calc 298.1438).

{$(DMP)_3$·L4}·3PF$_6$ (= **[4]PR4·3PF$_6$**). ^{1}H NMR (300 MHz, CD_3CN:$CDCl_3$) δ 8.77 (d, *J* = 9.0 Hz, 6H, H^a), 8.54 (d, *J* = 6.0 Hz, 6H, H^b), 7.36 (s, 3H, H^c), 7.11 (s, 3H, H^d), 6.86

(s, 10H, aryl-DMP), 4.89 (d, J = 13.6 Hz, 3H, H^e), 4.49 (t, J = 7.4 Hz, 6H, H^i), 3.79 (12H, m, H^f, H^g), 3.73 (30H, s, OMe-DMP), 3.70 (10H s, CH_2-DMP), 2.09 (6H, m, H^j), 1.33 (m, 12H, H^{k-o}), 0.88 (9H, t, J = 6.6 Hz, H^h). High-resolution Electrospray Mass spectrometry of $CD_3CN/CDCl_3$ solution of 1:3 **L4**·3PF_6 and DMP, showing formation of **[4]PR4**$^{3+}$ at m/z 1105.2059 (calc 1105.2157), along with {(DMP)$_2$·**L4**}$^{3+}$ at m/z 854.7674 (calc 854.7678), {(DMP)·**L4**}$^{3+}$ at m/z 604.6564 (calc 604.6543), and **L4**$^{3+}$ at m/z 354.2083 (calc 354.2064).

Molecular Modelling

The DMP macrocycle was manually placed on each side chain of the cavitand ligand and energy minimisation was performed using Macromodel [24] and the OPLS_2005 force field. [25] A chloroform solvent environment was used for the minimisation.

X-Ray Crystallography

Crystals were mounted under inert oil on a MiTeGen tip and flash frozen. X-ray diffraction data were collected using synchrotron radiation (λ= 0.6889 Å) at station I19 of Diamond Light Source (**L1**·3PF_6), or with Cu-K_α radiation (λ= 1.54184 Å) using an Agilent Supernova dual-source diffractometer with Atlas S2 CCD detector and fine-focus sealed tube generator (**L2**·3PF_6·2(CH_3CN)·2(H_2O)). Data were corrected for Lorenztian and polarization effects and absorption corrections were applied using multi-scan methods. The structures were solved by direct methods using SHELXS-97 and refined by full-matrix on F^2 using SHELXL-97.[26] Unless otherwise specified, all non-hydrogen atoms were refined as anisotropic, and hydrogen positions were included at geometrically estimated positions. Crystals of **L1**·3PF_6 were weakly diffracting. The refined structure contained significant void space with residual electron density which

could not be meaningfully modelled as either counter-anions nor solvent, hence the SQUEEZE routine of PLATON was employed.[27] $C_{48}H_{48}F_{18}N_3O_9P_3$, Mr = 1245.8, orange needle, 0.15 x 0.10 x 0.03 mm, monoclinic, a = 20.317(13), b = 24.489(17), c = 28.38(2) Å, β = 95.855(8), V = 14044(17) Å^3, space group $C2/c$, Z = 8, ρ_{calc} = 1.178 g cm^{-3}; λ = 0.68890 Å, θ_{max} = 24.25 °, 55535 data collected, R_{int} = 0.051, 547 parameters, R_1 = 0.1448 (for 7415 data $I > 2\sigma(I)$), wR_2 = 0.4499 (all 12238 data), T = 100(1) K. CCDC-1494001.

For (**L2**·3PF_6·2(CH_3CN)·2(H_2O) one **L2**$^{3+}$ cavitand cation was refined with two disordered group. One propyl group was refined with a methylene disordered across two positions each at 50% occupancy, and most of one *N*-propyl-pyridinium disordered over two positions at 75% and 25% occupancies. Disordered atoms, solvent water and acetonitrile positions were refined isotropically. $C_{110}H_{124}F_{33}N_{10}O_{20}P_6$, Mr = 2719.01, yellow prism, 0.20 x 0.11 x 0.06 mm, monoclinic, a = 32.7129(15), b = 20.3327(4), c = 40.5779(17) Å, β = 98.482(4), V = 26694.8(17) Å^3, space group $C2/c$, Z = 8, ρ_{calc} = 1.353 g cm^{-3}; λ = 1.54184 Å, θ_{max} = 70.00°, 48253 data collected, R_{int} = 0.0389, 1639 parameters, R_1 = 0.1623 (for 14453 data $I > 2\sigma(I)$), wR_2 = 0.4666 (all 20545 data), T = 110(1) K. CCDC-1494000.

Conclusions

Four novel pseudorotaxane systems have been synthesised as confirmed by ^{1}H NMR spectroscopy and mass spectrometry. These are the first examples of *tris*-substituted C_3-symmetric pseudorotaxanes formed from functionalised CTG-scaffolds, which themselves have host-like properties associated with the hydrophobic [*a.d.g*]cyclononatriene bowl. The affinity for alkyl-pyridinium units described in this work to assemble with pillar[5]arenes demonstrates the potential of this system for the

design of more complicated molecular machinery by incorporation of competing binding groups.

Acknowledgements

We thank the The Leverhulme Trust for funding (RPG-2014-148) and EPSRC for equipment funding (EP/K039202/1) and EPSRC and Charles Brotherton Trust for studentship support (JJH). We thank Tanya Marinko-Covell and Stephen Boyer for microanalysis. This work was carried out with support of Diamond Light Source (MT-10334). Data deposition http://doi.org/10.5518/123

References

(1) for recent reviews see (a) Cheng, C.; Stoddart, J. F. *ChemPhysChem* **2016**, *17*, 1780-1793; (b) Erbas-Cakmak, S.; Leigh, D. A.; McTernan, C. T.; Nussbaumer, A. L. *Chem. Rev.* **2015**, *115*, 10081-10206; (c) Evans, N. H.; Beer, P, D. *Chem. Soc. Rev.* **2014**, *43*, 4658-4683; (d) Neal, E. A.; Goldup, S. M. *Chem. Commun.* **2014**, *50*, 5128-5142; (e) van Dongen, S. F. M.; Cantekin, S.; Elemans, J. A. A. W.; Rowan, A. E.; Nolte, R. J. M. *Chem. Soc. Rev.* **2014**, *43*, 99-122; (f) Forgan, R. S.; Sauvage J.-P.; Stoddart, J. F. *Chem. Rev.* **2011**, *111*, 5434-5464; (g) Yang, W.; Li, Y.; Liu, H.; Chi, L.; Li. Y. *Small* **2012**, *8*, 504-516; (h) Durot, S.; Reviriego, F.; Sauvage, J.-P. *Dalton Trans.* **2010**, *39*, 10557-10570; (i) Kim, K. *Chem. Soc. Rev.* **2002**, *31*, 96-107.

(2) Xue, M.; Yang, Y.; Chi, X.; Yan, X.; Huang, F. *Chem. Rev.* **2015**, *115*, 7398-7501.

(3) Anelli, P. L.; Spencer, N.; Stoddart, J. F. *J. Am. Chem. Soc.* **1991**, *113*, 5131-5133.

(4) Badjić, J. D.; Balzani, V.; Credi, A.; Silvi, S.; Stoddart, J. F. *Science* **2004**, *303*, 1845-1849.

(5) (a) Jimenez-Molero, M. C.; Dietrich-Buchecker, C.; Sauvage, J.-P. *Chem. Commun.* **2003**, 1613-1616; (b) Liu, Y.; Flood, A. H.; Bonvallett, P. A.; Vignon, S. A.; Northrop, B. H.; Tseng, H.-R.; Jeppesen, J. O.; Huang, T. J.; Brough, B.; Baller, M.; Magonov, S.; Solares, S. D.; Goddard, W. A.; Ho, C.-M., Stoddart, J. F. *J. Am. Chem. Soc.* **2005**, *127*, 9745-9759.

(6) Meng, Z.; Chen, C.-F. *Chem. Commun.* **2015**, *51*, 8241-8244.

(7) for example (a) Viljoen, E.; Zhu, K.; Loeb, S. J. *Chem. Eur. J.* **2016**, *22*, 7479-7484; (b) Nikitin, K.; Müller-Bunz, H. *New J. Chem.* **2009**, *33*, 2472-2478.

(8) Ogoshi, T.; Kanai, S.; Fujinami, S.; Yamagishi, T.; Nakamoto, Y. *J. Am. Chem. Soc.* **2008**, *130*, 5022-5023.

(9) review Ogoshi, T.; Yamagishi, T. *Chem. Commun.* **2014**, *50*, 4776-4787.

(10) Zhou, Y.; Li, Z.; Chi, X.; Thompson, C.; Yao, Y. *Chem. Commun.* **2014**, *50*, 10482-10484.

(11) for example (a) Chi, X.; Xue, M.; Yao, Y.; Huang, F. *Org. Lett.* **2013**, *15*, 4722–4725; (b) Li, C.; Xu, Q.; Li, J.; Yao, F.; Jia, X. *Org. Biomol. Chem.* **2010**, *8*, 1568-1576; (c) Ogoshi, T.; Yamafuji, D.; Aoki, T.; Kitajima, K.; Yamagishi, T.; Hayashi, Y.; Kawauchi, S. *Chem. Eur. J.* **2012**, *18*, 7493-7500; (d) Ogoshi, T.; Yamafuji, D.; Yamagishi, T.; Brouwer, A. M. *Chem. Commun.* **2013**, *49*, 5468-5470.

(12) (a) Manoni, R.; Neviani, P.; Franchi, P.; Mezzina, E.; Lucarini, M. *Eur. J. Org. Chem.* **2014**, 147-151; (b) Kitajima, K.; Ogoshi, T.; Yamagishi, T. *Chem. Commun.* **2014**, *50*, 2925-2927; (c) Ogoshi, T.; Kayama, H.; Yamafuji, D.; Aoki, T.; Yamagishi, T. *Chem. Sci.* **2012**, *3*, 3221.

(13) (a) Tokunaga, Y.; Kimura, M.; Ueda, M.; Miyagawa, S.; Kawasaki, T.; Hisada, K. *Tetrahedron Lett.* **2016**, *57*, 1120-1123; (b) Li, H.; Li, X.; Ågren, H.; Qu, D.-H. *Org. Lett.* **2014**, *16*, 4940-4943; (c) Zhang, J.-N.; Li, H.; Zhou, W.; Yu, S.-L.; Qu, D.-H.;

Tian, H. *Chem. Eur. J.* **2013**, *19*, 17192-17200; (d) Hsueh, S.-Y.; Cheng, K.-W.; Lai, C.-C.; Chiu, S.-H. *Angew. Chem. Int. Ed.* **2008**, *47*, 4436-4439; (e) Leung, K. C.-F.; Aricó, F.; Cantrill, S. J.; Stoddart, J. F. *J. Am. Chem. Soc.* **2005**, *127*, 5808-5810; (f) Gibson, H. W.; Yamaguchi, N.; Hamilton, L.; Jones, J. W. *J. Am. Chem. Soc.* **2002**, *124*, 4653-4665; (g) Amabilino, D. B.; Ashton, P. R.; Bělohradský, M.; Raymo, F. M.; Stoddart, J. F. *J. Chem. Soc., Chem. Commun.* **1995**, 751-753.

(14) Tokunaga, Y.; Ito, T.; Sugawara, H.; Nakata, R. *Tetrahedron Lett.* **2008**, *49*, 3449-3452.

(15) Loeb, S. J.; Tramontozzi, D. A. *Org. Biomol. Chem.* **2005**, *3*, 1393-1401.

(16) Collet, A. *Tetrahedron* **1987**, *43*, 5725-5759.

(17) (a) Brotin, T.; Guy, L.; Martinez, A.; Dutasta, J.-P. *Top. Curr. Chem.* **2013**, *341*, 177-230; (b) Hardie, M. J. *Chem. Soc. Rev.* **2010**, *39*, 516-527; (c) Brotin, T.; Dutasta, J-P. *Chem. Rev.* **2009**, *109*, 88-130.

(18) Henkelis, J. J.; Hardie, M. J. *Chem. Commun.* **2015**, *51*, 11929-11943.

(19) (a) Rudzevich, Y.; Rudzevich, V.; Böhmer, V. *Chem. Eur. J.* **2010**, *16*, 4541-4549; (b) Bogdan, A.; Rudzevich, Y.; Vysotsky, M. O.; Böhmer, V. *Chem. Commun.* **2006**, 2941-2952; (c) Gaeta, C.; Vysotsky, M. O.; Bogdan, A.; Böhmer, V. *J. Am. Chem. Soc.* **2005**, *127*, 13136-13137.

(20) Hardie, M. J.; Sumby, C. J. *Inorg. Chem.* **2004**, *43*, 6872-6874.

(21) Thorp-Greenwood, F. L.; Ronson, T. K.; Hardie, M. J. *Chem. Sci.* **2015**, *6*, 5779-5792.

(22) (a) Song, J.; Shi, Y.; Huang, Z.; Zheng, Q. *Chin. J. Chem.* **2015**, *33*, 765-770; (b) Yu, J.-T.; Huang, Z.-T.; Zheng, Q.-Y. *Org. Biomol. Chem.* **2012**, *10*, 1359-1364; (c) Henkelis, J. J.; Barnett, S. A.; Harding, L. P.; Hardie, M. J. *Inorg. Chem.* **2012**, *51*, 10657-10674; (d) Little, M. A.; Ronson, T. K.; Hardie, M. J. *Dalton Trans.* **2011**, *40*,

12217-12227; (e) Shi, Y.-Y.; Sun J., Huang, Z.-T.; Zheng, Q.-Y. *Cryst. Growth Des.* **2010**, *10*, 314-320; (f) Carruthers, C. J.; Ronson, T. K.; Sumby, C. J.; Westcott, A.; Harding, L. P.; Prior, T. J.; Rizkallah, P.; Hardie, M. J. *Chem. Eur. J.* **2008**, *14*, 10286-10296; (g) Hu, Q.-P.; Ma, M.-L.; Zheng, X.-F.; Reiner, J.; Su, L. *Acta Crystallogr., Sect. E*, **2004,** *60*, o1178.

(23) for example (a) Wei, W.; Wang, G.; Zhang, Y.; Jiang, F.; Wu, M.; Hong, M. *Chem. Eur. J.* **2011**, *17*, 2189-2198; (b) Makha, M.; Raston, C. L.; Sobolev, A. N. *Aust. J. Chem.*, 2006, **59**, 260-262; (c) Brouwer, E. B.; Udachin, K. A.; Enright, G. D.; Ripmeester, J. A.; Ooms, K. J.; Halchuk, P. A. *Chem. Commun.* **2001**, 565-566.

(24) Schrödinger Release 2014-2: MacroModel, version 10.4, Schrödinger, LLC, New York, NY, 2014.

(25) Shivakumar, D.; Williams, J.; Wu, Y.; Damm, W.; Shelley, J.; Sherman, W *J. Chem. Theory Comput.* **2010**, *6*, 1509–1519.

(26) Sheldrick, G. M. *Acta Crystallogr. A* **2008**, *A64*, 112-122.

(27) Van der Sluis, P.; Spek, A. L. *Acta Crystallogr. A* **1990**, *A46*, 194-201.